AD-A085 887 MASSACHUSETTS INST OF TECH CAMBRIDGE DEPT OF MATERIA--ETC F/6 11/6
A STEM ANALYSIS OF TWO RAPIDLY SOLIDIFIED STAINLESS STEELS.(U)
MAR 80 T F KELLY, J B VANDER SANDE N00014-76-C-0171
UNCLASSIFIED NL

END
DATE FILMED
8-80
DTIC

UNCLASSIFIED

SECURITY CLASSIFICATION OF THIS PAGE (When Data Entered)

(1)

REPORT DOCUMENTATION PAGE	READ INSTRUCTIONS BEFORE COMPLETING FORM
1. REPORT NUMBER: 6 — 2. GOVT ACCESSION NO.: AD-A085887	3. RECIPIENT'S CATALOG NUMBER
4. TITLE (and Subtitle): A STEM Analysis of Two Rapidly Solidified Stainless Steels	5. TYPE OF REPORT & PERIOD COVERED: Technical Report Oct. 1978 to Jan. 1980
	6. PERFORMING ORG. REPORT NUMBER
7. AUTHOR(s): T. F. Kelly and J. B. VanderSande	8. CONTRACT OR GRANT NUMBER(s): N00014-76-C-0071, NR031-795
9. PERFORMING ORGANIZATION NAME AND ADDRESS: Massachusetts Institute of Technology Cambridge, Massachusetts 02139	10. PROGRAM ELEMENT, PROJECT, TASK AREA & WORK UNIT NUMBERS
11. CONTROLLING OFFICE NAME AND ADDRESS: Office of Naval Research Arlington, Virginia 22217	12. REPORT DATE: March 25, 1980
	13. NUMBER OF PAGES: 12
14. MONITORING AGENCY NAME & ADDRESS (if different from Controlling Office)	15. SECURITY CLASS. (of this report): Unclassified
	15a. DECLASSIFICATION/DOWNGRADING SCHEDULE

16. DISTRIBUTION STATEMENT (of this Report)

Unlimited

17. DISTRIBUTION STATEMENT (of the abstract entered in Block 20, if different from Report)

18. SUPPLEMENTARY NOTES

To be published in Proceedings of the 2nd Conference on Rapid Solidification Processing Principles and Technologies, Reston, Virginia, March 23-26, 1980.

19. KEY WORDS (Continue on reverse side if necessary and identify by block number)

Rapid Solidification Processing
Austenitic stainless steels
Scanning transmission electron microscopy

20. ABSTRACT (Continue on reverse side if necessary and identify by block number)

Scanning transmission electron microscopy (STEM) has been used for microstructural and microchemical analysis of two rapidly solidified austenitic stainless steels. One steel is a high-sulfur, 303 stainless type. In this rapidly solifified steel, sulfide particles (MnS) are found to be two or three orders of magnitude smaller in size, and more uniformly distributed, than in the conventionally processed material. Extremely small sulfide particles have been observed at the cell walls and in the intra-

DD FORM 1 JAN 73 1473 EDITION OF 1 NOV 65 IS OBSOLETE

SECURITY CLASSIFICATION OF THIS PAGE (When Data Entered)

DISCLAIMER NOTICE

THIS DOCUMENT IS BEST QUALITY PRACTICABLE. THE COPY FURNISHED TO DTIC CONTAINED A SIGNIFICANT NUMBER OF PAGES WHICH DO NOT REPRODUCE LEGIBLY.

cellular region of the solidification structure of individual rapidly solidified powder particles. Moreover, composition profiles have been obtained by the STEM across regular and nonregular cell walls in these powders which indicate that a high degree of chemical homogeneity has obtained. A comparison is made of the microstructures and microchemistry of individual powders, consolidated powder product, and conventionally processed versions of this high-sulfur austenitic stainless steel.

The rapidly solidified powders of a high-phosphorus stainless steel have also been observed in STEM. The results of these observations are presented in light of the data obtained on the high-sulfur steel.

A STEM ANALYSIS OF TWO RAPIDLY SOLIDIFIED STAINLESS STEELS

T. F. Kelly and J. B. Vander Sande

Department of Materials Science and Engineering
Massachusetts Institute of Technology
Cambridge, Massachusetts

(15) N00014-76-C-0171

(11) 26 Mar 80

(9) Technical Rept., Oct. 77-Jan 80,

no. 6,

ABSTRACT

Scanning transmission electron microscopy (STEM) has been used for microstructural and microchemical analysis of two rapidly solidified austenitic stainless steels. One steel is a high-sulfur, 303 stainless type. In this rapidly solidified steel, sulfide particles (MnS) are found to be two or three orders of magnitude smaller in size, and more uniformly distributed, than in the conventionally processed material. Extremely small sulfide particles have been observed at the cell walls and in the intracellular region of the solidification structure of individual rapidly solidified powder particles. Moreover, composition profiles have been obtained by the STEM across regular and non-regular cell walls in these powders which indicate that a high degree of chemical homogeneity has obtained. A comparison is made of the microstructures and microchemistry of individual powders, consolidated powder product, and conventionally processed versions of this high-sulfur austenitic stainless steel.

The rapidly solidified powders of a high-phosphorus stainless steel have also been observed in STEM. The results of these observations are presented in light of the data obtained on the high-sulfur steel.

INTRODUCTION

Rapid solidification processing (RSP) has been viewed[1] as a means of obtaining better properties from (crystalline) metal alloys. Improvements in properties are largely a result of the following effects of high cooling rates on the "as solidified" structure of crystalline metal alloys: a) reduced segregate spacing with increased cooling rates; b) reduced solute segregation levels (solute trapping) and/or segregationless solidification; c) suppression of stable phase formation and/or retention of metastable phases. Primarily as a result of a), direct chemical observation of such effects as b) and c) in RSP alloys has been limited. With the advent of the dedicated scanning transmission electron microscope (STEM), the capability for compositional analysis by X-ray fluorescence spectroscopy with a spatial resolution on the order of 50 Å in thin sections has been realized. Microchemical information with this resolution from RSP alloys, with the associated microstructural images, should lead to a better understanding of the processes occurring during solidification of alloys at high cooling rates. Such microchemical information is likewise important to the development of consolidation techniques that can optimize the advantage gained in RSP. Development of this fundamental understanding of the process cycle is crucial for future success in realization of RSP as a technologically and economically viable processing option.

The motivation for development of a type 303 stainless steel* was the need for producing a "free machining" grade of stainless steel. By addition of large amounts of sulfur ($\gtrsim$ 0.15 wt%) in combination with manganese, a brittle second-phase manganese sulfide is formed which aids the formation of small chips during machining operations. Hence, type 303 stainless steel is a high sulfur, free-machining grade of austenitic stainless steel. This investigation has attempted to ascertain the effects of rapid solidification processing on the microstructure and microchemistry of 303 stainless steel and compare the RSP product with an equivalent conventionally processed 303 stainless steel. A high-phosphorus stainless steel** RSP powder has also been studied and some results of this work are presented.

EXPERIMENTAL PROCEDURE

The RSP material studied in this investigation was prepared*** by forced convective cooling, in helium, of centrifugally atomized metal droplets to achieve cooling rates on the order of 10^5°C/sec. The resultant powder, which consists of spherical particles in the range 5 to 200 microns diameter, was sieved to -140 mesh, enclosed in a stainless steel can and consolidated to a fully dense, one-inch diameter rod by hot extrusion at 900°C and a 10:1 reduction ratio. Equivalent conventionally processed 303 stainless steel was obtained from Carpenter Technology Corporation who had originally requested the rapid solidification processing run. The conventionally processed material was prepared by hot rolling of a cast 12-inch diameter ingot down to 3½-inch diameter bar stock. The 303 stainless steel of this investigation was therefore studied in three processed states: the rapidly solidified powder, the rapidly solidified and consolidated bar stock, and the conventionally processed material.

Preparation of thin specimens of the "as solidified" powder particles was accomplished using a modified version of the technique described by Field and Fraser.[2] The metal powder is mixed with an equal weight of plastic cement and the mixture is poured onto a flat surface (polished metal or teflon) to harden. The flat surface of the resulting coupon is polished lightly on a 0.3 μ alumina wheel to expose metal particles and nickel is electrodeposited onto this flat

*Nominal composition as determined by Carpenter Technologies Corporation:

Cr	Ni	Mn	Cu	Si	Mo	S	Co	C	N	P	Fe
17.31	8.68	1.60	0.78	0.62	0.37	0.34	0.15	0.059	0.032	0.028	bal.

**Nominal composition:

Cr	Ni	P	C	Fe
15.0	9.7	0.42	0.34	bal.

***The powders were kindly supplied by Pratt and Whitney Aircraft Group, United Technologies Corporation, West Palm Beach, Florida.

surface to a thickness of about 0.075 mm. The "Watts" type nickel plating bath contained 330 g/l $NiSO_4 \cdot 4H_2O$; 60 g/l $NiCl_2 \cdot 6H_2O$; 40 g/l H_3BO_4; 0.5 g/l wetting agent (sodium lauryl sulfate), and was operated at 45 to 65°C, pH 4.0 to 5.5 with $\lesssim$ 0.03 amp/cm^2. It may be necessary to first evaporate some nickel onto the surface to make it electrically conductive. After electroplating, the plastic cement is dissolved in acetone. The resulting foil can be chemically cleaned in 50 ml H_2O_2 with a few drops of HF. It is imperative that the final composite foil be clean and free from any contamination and this intermediate cleaning step should be considered carefully. The second side is then electroplated with nickel to form a sandwich of metal powders in electroplated Ni. Three-millimeter diameter discs can be punched from this composite foil and electropolished in a conventional way. In this work, a twin-jet Fischione electropolishing unit was used with 20% perchloric/methanol at -50°C and 20 to 30 volts or about 0.4 amps/cm^2.

One source of difficulty in this technique is the unequal electropolishing rates of the electrodeposited metal and powder specimen material. In this study, the electrodeposited nickel dissolved at a slightly faster rate than the 303 stainless steel powder and therefore few usable specimens were obtained by electropolishing. The unsuccessful electropolished specimens were, however, final thinned on a routine basis using an ion thinning apparatus. Thin specimens of the RSP consolidated material and the conventionally processed material were prepared by the electropolishing techniques above.

RESULTS

Microstructures

The most striking feature of the microstructure of a conventionally processed 303 stainless steel is the presence of large (100 microns long by 20 microns wide) precipitates of cigar-like shape strung out in the rolling direction of the material, Figure 1. These are the larger precipitates in a size distribution where the lower limit is about 1-micron diameter.

The precipitate morphology of the RSP powder material shows a marked difference from that of the conventionally processed material, Figure 2. The largest precipitates are generally 1000 to 2000 Å diameter and equiaxed. These are observed to be arranged in the structure in a cellular network. That is, they appear to reside on the cell walls of the solidification structure and hence appear to outline the cellular structure. A smaller (100 to 500 Å diameter) equiaxed precipitate is also often observed dispersed throughout the intracellular region of the structure, Figs. 2, 5, and 12. These are present seemingly independent of the larger (1000 to 2000 Å) precipitates at the cell walls. In fact, powder particles have been observed in TEM and STEM which contain no large (1000 to 2000 Å) precipitates and have no apparent cell structure, yet the small (100 to 500 Å) precipitates were present in a uniform dispersion throughout the material, Fig. 3. Powder particles with no apparent cellular structure have also been observed in standard metallurgical sections. In particular, the smaller diameter powder particles (~ 20-micron diameter) are more frequently observed to lack cellular structure.

The consolidation process (hot extrusion) appears not to have a significant effect on the number, size, and shape of these precipitates in the RSP material, Fig. 4. It appears that the hot extrusion deforms primarily the austenite and, hence,

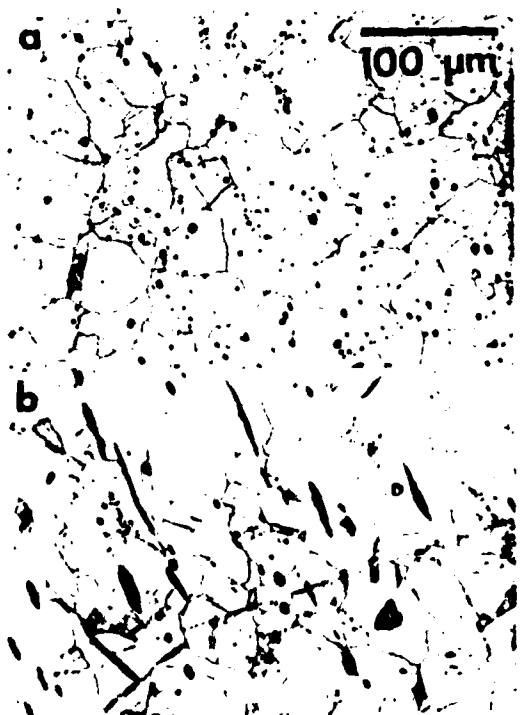

Fig. 1. Conventionally processed 303 stainless steel. Light microscope image of a) transverse and b) longitudinal section.

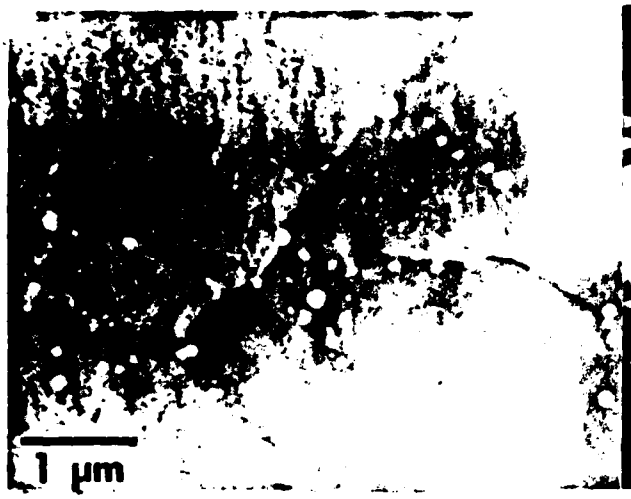

Fig. 2. 303 stainless steel RSP powder with non-regular cellular structure. STEM annular dark field image.

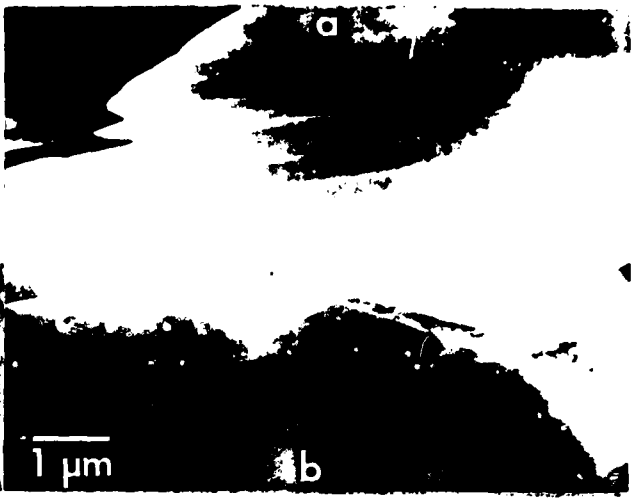

Fig. 3. 303 stainless steel RSP powder. STEM annular dark field image of both a) a non-cellular powder and b) a cellular powder.

changes only the spatial arrangement of the precipitates although it is possible that some coarsening of the precipitate does occur. Note especially that the small (100 to 500 Å) precipitates are retained. Thus, a comparison of the RSP consolidated product with the conventionally processed material shows a reduction in size of two to three orders of magnitude with a corresponding uniform dispersion of the precipitate in the RSP consolidated product.

The effect of RSP on the grain structure of the material has been studied. The conventionally processed material exhibits a partially annealed grain structure with annealing and/or deformation induced twins evident and with a 30 micron average grain size in the as-hot-rolled condition, Fig. 1. The grain structure of the RSP powder particles appears to be dependent on the solidification mode. Most of the powder particles observed in TEM had a non-regular cell structure within the confines of small ($\lesssim$ 5 μm) grains, Fig. 2. The grain boundaries were found, in general, to be of high angle character by selected area electron diffraction observations. Misorientation across cell walls of a single grain was generally not observed in the 303 stainless steel but in some cases low angle boundaries were observed, Fig. 5. Two additional types of solidification structure were observed, both of less frequent occurrence relative to the above type of structure. A regular cellular solidification structure (possibly dendritic) was observed as evidenced by the cellular arrangement of precipitates and the large extent of the single grain that contained the cells, Fig. 6. Chemical evidence for this (see Fig. 1[illegible]) has also been obtained. As mentioned previously,

Fig. 4. 303 stainless steel RSP consolidated. TEM bright field image.

Fig. 5. 303 stainless steel RSP powder. STEM bright field image. Non-regular cellular structure.

a non-cellular structure has been observed. No grain boundaries were apparent in any observations of this last structure.

It is instructive to compare these observed structures to that of a high phosphorus stainless steel RSP powder, Fig. 7. This is a clear case of a cellular structure (possibly dendritic) where the cell walls are lined with a continuous second phase. Microdiffraction was used to determine that the second phase lining the cell walls is amorphous. Microdiffraction was also used to determine that each of the cells is part of the same grain with only slight changes in orientation between cells as evidenced by Kikuchi lines in the microdiffraction pattern. Electron energy loss spectroscopy analysis of the second phase was obtained with the expectation of observing large amounts of carbon in the form of phosphocarbides. In fact, it was observed that there was no noticeable difference in carbon levels between the second phase and the matrix but that there is a large amount of chromium and little nickel present in the second phase relative to the matrix. The "hexagonal" arrangement of these cells was observed in several areas and a linearly arranged structure (which may be a longitudinal section of a cell), Fig. 16, was also observed.

Fig. 6. 303 stainless steel RSP powder. a) TEM bright field montage and b) STEM annular dark field of same area. Regular cellular structure.

Observations of the surfaces of the powder particles using scanning electron microscopy (SEM) revealed information that is consistent with the above observations. Principally, no dendritic or regular cellular structure was observed on the 303 stainless steel RSP powder surfaces (Fig. 8a is a typical example). There are areas on the surface that have a cellular appearance, but continuity of the cellular network is lacking. Figure 8b shows a smaller powder particle that must have collided with a larger, still partially molten, powder particle. Note the smooth surface of the smaller powder particle, especially as compared with the larger particle. These structures can be contrasted with the dendritic appearance of the high phosphorus stainless steel RSP powder, Fig. 8c. All of the high phosphorus powder particles observed in SEM had such a dendritic appearance.

A duplex grain structure is observed in the as-extruded, RSP consolidated material. This consists of larger ($\sim$ 5 to 10 microns) grains surrounded by small ($\lesssim$ 1 micron), more heavily dislocated grains, Fig. 4. It is not clear whether the larger grains have recrystallized from deformed grains or whether the larger grains simply did not deform during hot extrusion. It may be that the answer is a combination of these two possibilities, i.e., the larger grains deformed less during hot extrusion and subsequently recrystallized to the observed state. An annealing treatment of 1000°C for 1 hour effected some recovery of the structure; however, in some regions dislocation networks remained, Fig. 9. A comparison of grain growth characteristics of the conventionally processed material and the RSP consolidated material was obtained by measurement of the average grain size at each of three annealing temperatures, 1000°C, 1100°C, and 1200°C. The results are shown in Fig. 10. The grain growth behavior of the conventional material appears to be "normal" while that of the RSP consolidated material is retarded, especially for the higher temperatures.

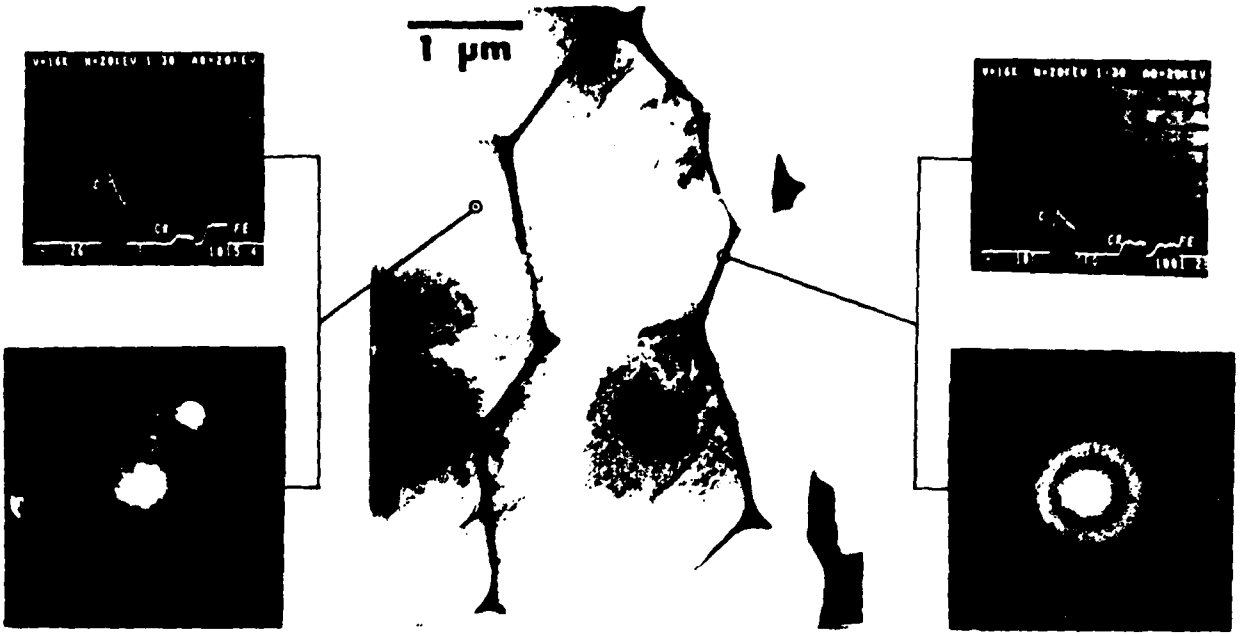

Fig. 7. High phosphorus stainless steel RSP powder. STEM bright field image with microdiffraction patterns and electron energy loss spectra from the indidated points. The peaks for C, Cr, and Fe (after background subtraction) are labeled.

Microchemistry

The microchemical nature of each of the three process states of the 303 stainless steel has been studied. Figure 11 is an example of a single spectrum taken from a precipitate in the RSP powder. It identifies the precipitates as nominally manganese sulfides. Both the large (1000 to 2000 Å) and the small (100 to 500 Å) precipitates in both the RSP powder and the RSP consolidated material were identified, similarly, as manganese sulfides.

Composition profiles across features of interest in each material were generated by point-by-point collection of X-ray fluorescence spectra at appropriate spacings in the structure. The $K\alpha$ peak intensity (normalized to FeK_α) of chromium, nickel, and sulfur is plotted for each spectrum of the profile. A composition profile across a grain boundary in a powder particle typical of the non-regular cell structure type is shown in Figure 12. There is essentially no chemical variation across the grain boundary. Note that the profile does extend into the middle of the apparent cell on either side of the boundary. Another non-regular cellular structure of an RSP powder particle with associated composition profile is shown in Figure 13. The supposed cell walls of this

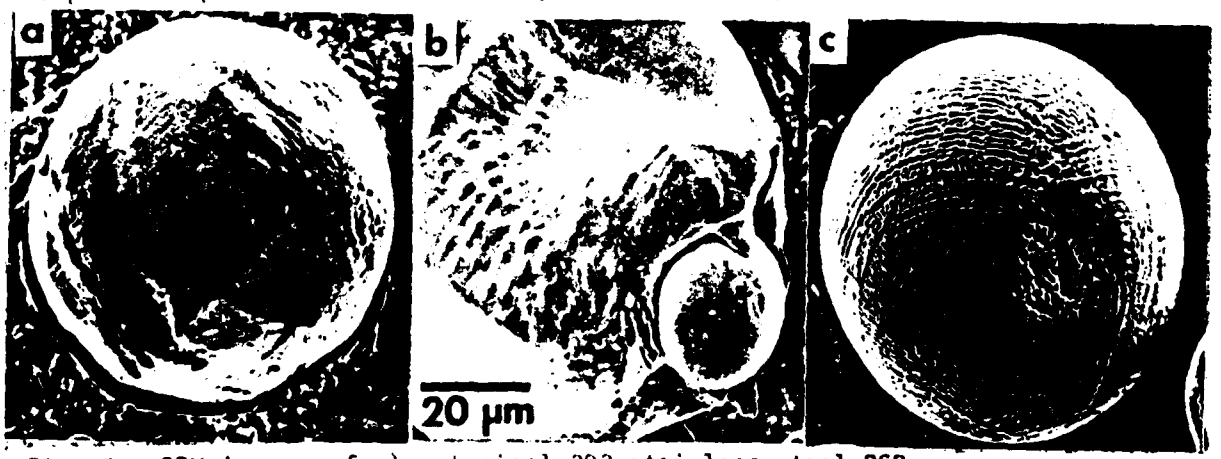

Fig. 8. SEM images of a) a typical 303 stainless steel RSP powder particle, b) a smaller 303 stainless steel RSP powder particle embedded in a larger one, c) a typical high phosphorus stainless steel RSP powder particle.

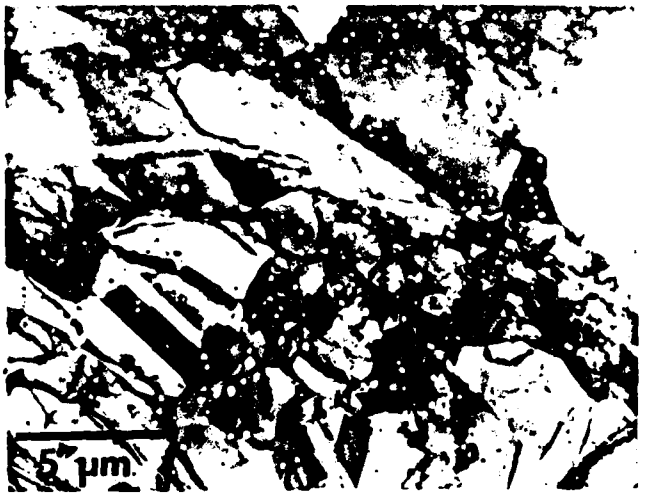

Fig. 9. 303 stainless steel RSP consolidated. Annealed for 1 hour at 1000°C. TEM bright field.

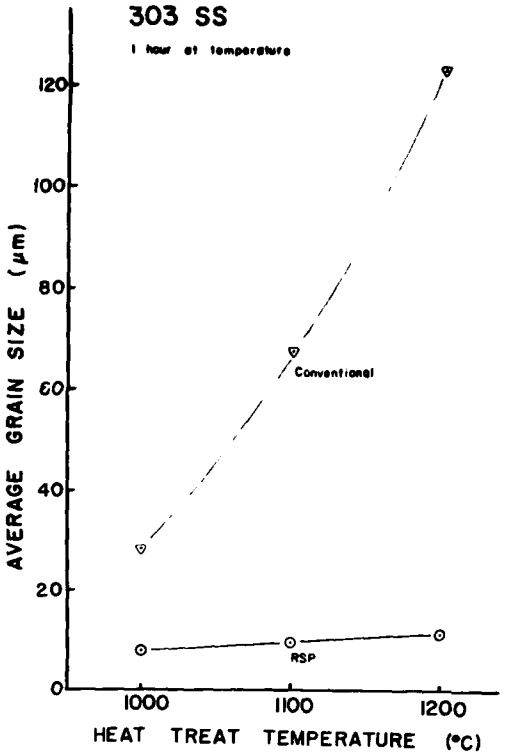

Fig. 10. Grain growth behavior comparison between 303 stainless steel conventionally processed and RSP consolidated.

sample as delineated by the precipitates do not seem to be correlated with the apparent grain boundaries. The composition profile was taken, as indicated, across a cell wall and up to a grain boundary. No large variation in chemistry was observed, although it appears that nickel and sulfur are slightly higher in composition near the cell wall. Note, this is one of the few samples that was thinned to electron transparency solely by electropolishing techniques. A composition profile across a cell wall of the apparent dendritic structure of Fig. 6 is shown in Fig. 14. There does appear to be some enrichment in chromium, nickel, and sulfur at the cell wall, which is consistent with the supposition of a dendritic (or cellular) structure. It should be noted that the degree of enrichment indicated here is not very large. Overall, the amount of segregation observed in the RSP powder was very low and, indeed, was limited to the above observation of segregation in a dendritic structure.

Since there is no cell structure in either the RSP consolidated material or the conventionally processed material, the grain structure is used as a basis about which a composition profile can be oriented. A composition profile that starts near the edge of a large recrystallized grain in the RSP consolidated material and continues into the small grain region is shown in Figure 15. Here again, no segregation of chromium, nickel, or sulfur is observed, but some

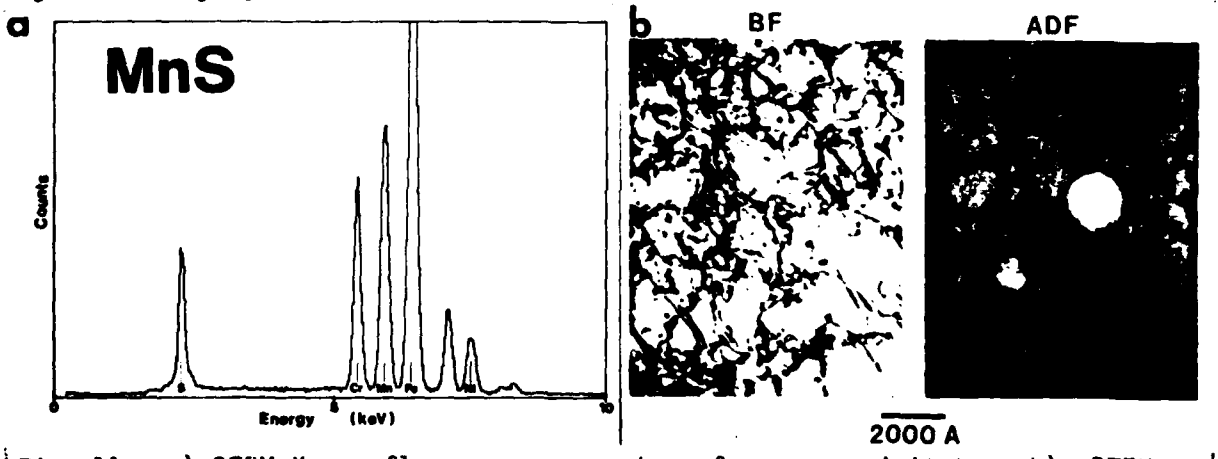

Fig. 11. a) STEM X-ray fluorescence spectrum from a precipitate. b) STEM bright field (BF) and STEM annular dark field (ADF) images of same field of view in 303 stainless steel RSP powder.

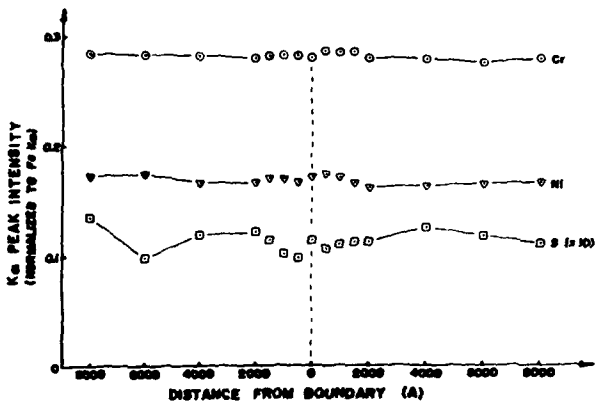

Fig. 12. 303 stainless steel RSP powder, non-regular cellular structure and associated composition profile. Arrow indicates direction of profile.

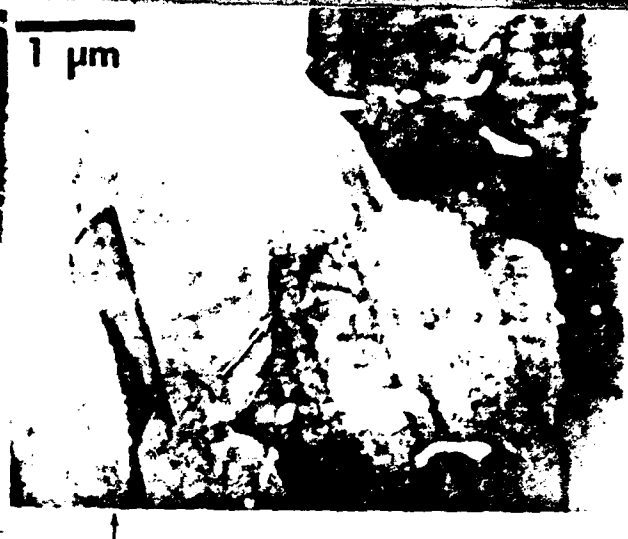

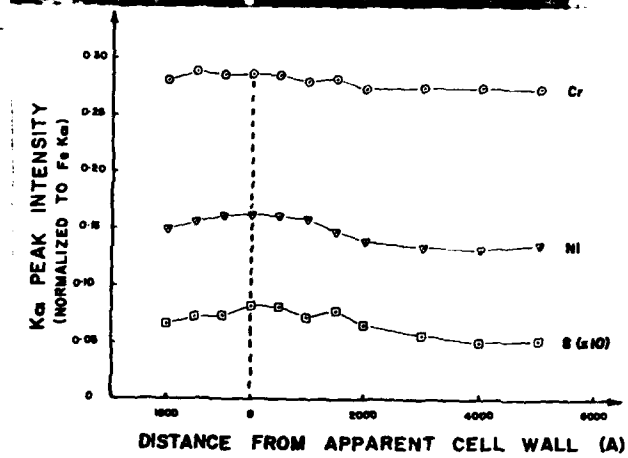

Fig. 13. 303 stainless steel RSP powder, non-regular cellular structure and associated composition profile. Arrow indicates direction of profile.

variation in silicon was observed in the small grain region. A composition profile across a grain boundary of the conventionally processed material was obtained with the expectation that segregation might be more prominent in this structure. The profile with a total extent of 5 microns showed no variation in chromium or nickel. Both sulfur and silicon did show a noticeable decrease 1000 Å ahead of the grain boundary and an equal increase 1000 Å after the grain boundary, but this was the only activity associated with these elements.

The high phosphorus stainless steel was examined next since, it was reasoned, phosphorus has a higher propensity for segregating in steels than does sulphur. The composition profile of Figure 16 shows significant segregation of chromium, nickel, and phosphorus at the cell wall of a longitudinal section of a cell. Note the rapid decrease of the phosphorus signal (and indeed the nickel and chromium signals) within 500 Å of the cell wall. Electron energy loss spectroscopy analysis of the second phase was obtained with the expectation of observing large amounts of carbon in the form of phosphocarbides. In fact, it was observed that there was no noticeable difference in carbon levels between the second phase and the matrix but that there is a large amount of chromium and little nickel present in the second phase relative to the matrix. A profile was obtained across a cell wall at which a discontinuity in the second phase existed so that the profile intercepted no second phase. Chromium, nickel, and phosphorus all increased somewhat at the boundary, similar to the nickel behavior in Fig. 17 but there was no "spike" in the profile at the boundary for either chromium or phosphorus.

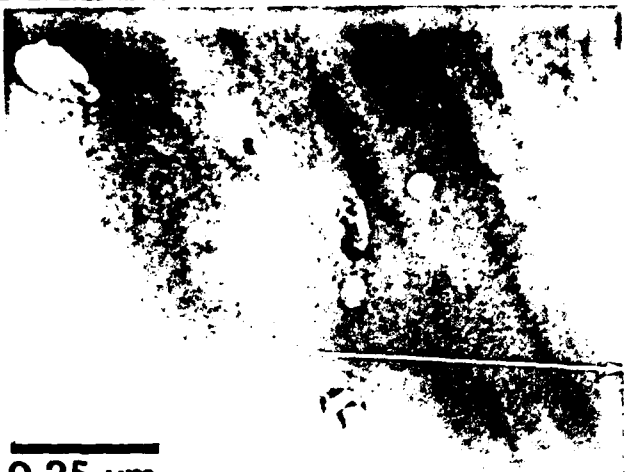

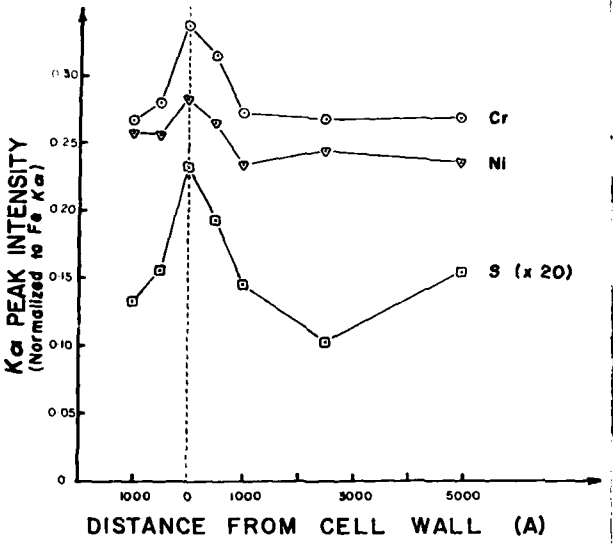

Fig. 14. 303 stainless steel RSP powder, regular cellular structure, and associated composition profile. Arrow indicates direction of profile.

Fig. 15. (Top) 303 stainless steel RSP consolidated material and (below) associated composition profile. Arrow indicates direction of profile. Two grain boundaries were traversed as indicated by dashed lines in plot.

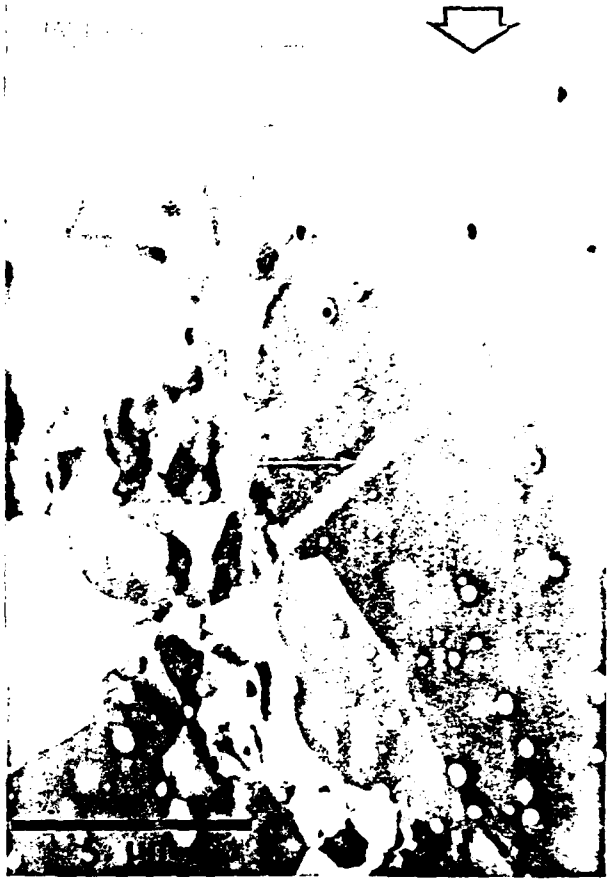

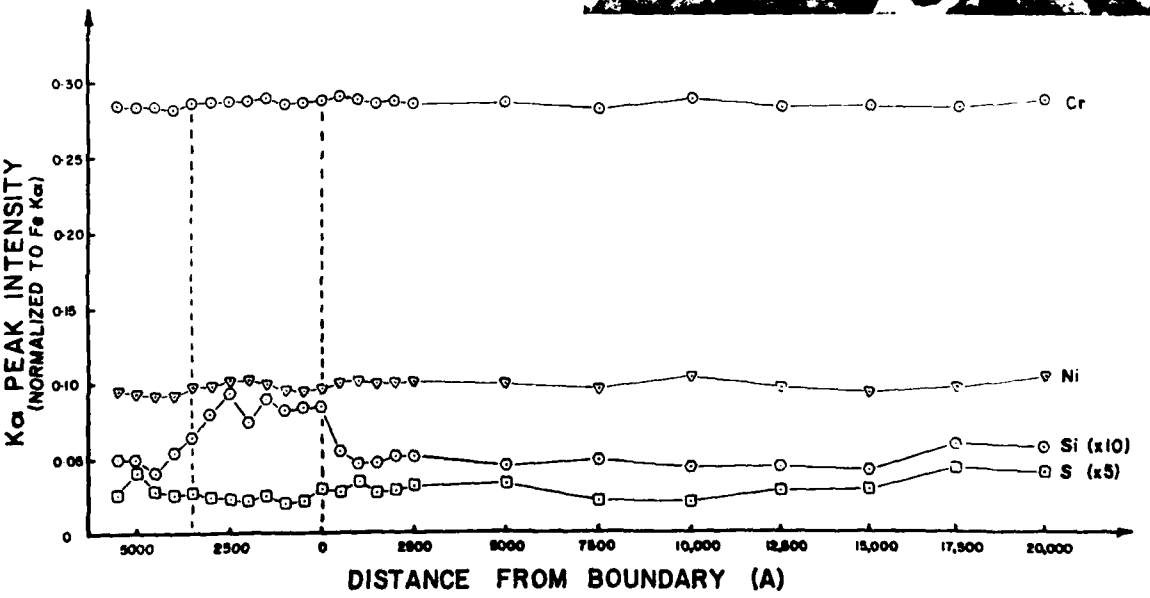

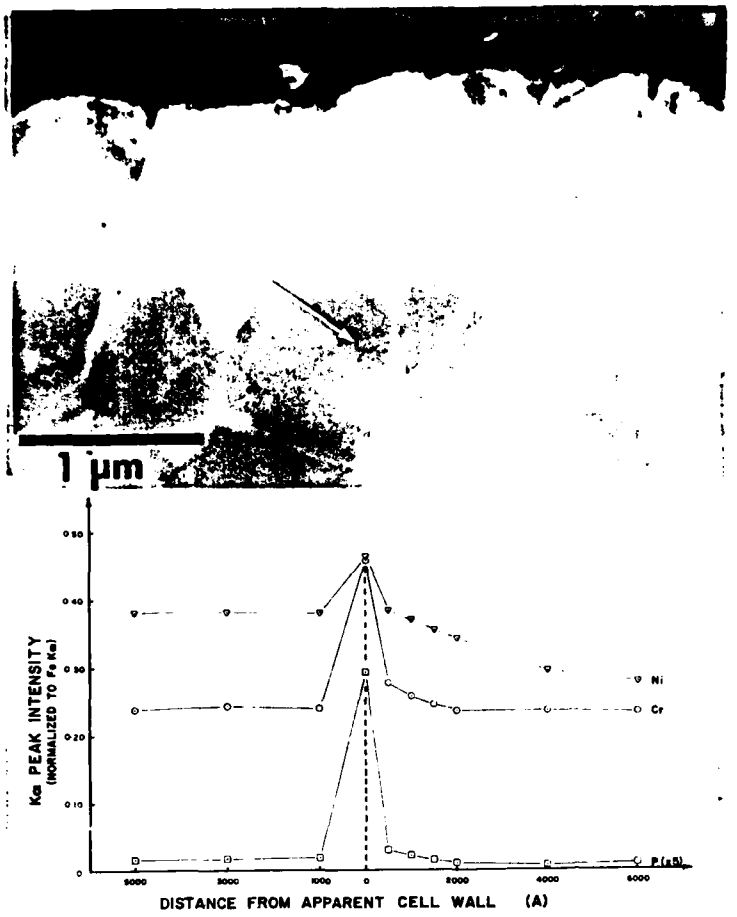

Fig. 16. High phosphorous stainless steel RSP powder, longitudinal section of cell structure, and associated composition profile. Arrow indicates direction of profile.

V. DISCUSSION

It is instructive to consider the microstructural and microchemical information gathered here in terms of the current understanding of solidification phenomena, both to enhance appreciation of the structures and to ascertain its place among current theories. It is probable that the large cigar-shaped precipitates of the conventionally processed material are the deformed remnants of large equiaxed precipitates that would form in the later stages of dendritic solidification from the solute rich interdendritic fluid. Similarly, in the structure of the cellular RSP material, the larger (1000 Å to 2000 Å) precipitates would have formed from a solute rich fluid in the later stages of cellular solidification, the size and separation of the precipitates being scaled to the finer cell size of the RSP material. Then, the presence of the large ($\gtrsim$ 1000 Å) precipitates in the RSP powder material indicate the prior existence of a solute enriched intercellular fluid, richer at least in the species that eventually comprise the precipitates. The higher the degree of enrichment of the intercellular fluid, the greater should be the volume of precipitates that form from that fluid.

In less-than-rapid solidification of an alloy, the degree of enrichment of the intercellular fluid is nearly constant over wide ranges of solidification rate; the cell spacing merely decreases as solidification rate increases. At rapid solidification rates, however, solute trapping at the advancing solid-liquid interface may occur. Note then the number density of precipitates present at the cell walls in the dendritic (or regular cellular) structure of Fig. 7 and compare it with that of the non-regular cellular structure of Fig. 2. It appears that there is a noticeably higher number of precipitates at the cell wall of the dendritic structure. Note also that the non-regular cell structure has a significant number of small (100 Å to 500 Å) intracellular precipitates whereas the dendritic structure has none. This effect can be explained by some degree of solute trapping in the early stages of cellular growth (central portion of cell) with perhaps a lesser degree of solute trapping or none at all in the later stages of cell growth. This would result in a less enriched intercellular

fluid from which fewer large (≳ 1000 Å) precipitates would form. It would also leave a supersaturated solid solution in the intracellular region from which the small (100 to 500 Å) precipitates would form on cooling. Within this interpretation, it seems that Fig. 5 is a more extreme case of the solute trapping. The number density of intercellular precipitates is low while the number density of small intracellular precipitates is high.

The origins of the cellular structures can be considered in light of these observations on the precipitate morphologies. It is possible to describe a process scenario that allows for development of each of the solidification structures observed. With the high cooling rates in the convective cooling of the liquid metal droplets, large supercoolings can obtain prior to nucleation. If this degree of supercooling is sufficient to enter a regime where copious nucleation ensues (either heterogeneous or homogeneous), then many independent grains should develop. Based simply on spatial constraints, a regular cellular structure would likely not develop if the grain size is on the order of, or even significantly larger than, the cell size. In addition, at the large supercooling, growth of the crystal would be rapid and the tendency should be toward a spherical front or stunted cellular growth.[3,4] Also, in this regime of large supercooling of the liquid, solute trapping can be expected.[5]

The observation of small grained, non-regular cell structures is compatible with the above description. The observations on the precipitate morphologies that indicate possible solute trapping and subsequent solid state precipitation from a supersaturated solution supports the supposition of large supercoolings of the liquid. In addition, the chemical profiles in the non-regular cell structures indicate nil segregation (except that associated with the precipitates). Note also that, within this scenario, a regular cellular structure (which has been observed) is merely a less likely possibility. The presence of the non-cellular structure appears to be associated with the smaller size (≲ 30 microns) powder particles. This can be interpreted as indicating that higher cooling rates are needed to obtain this structure but, in addition, smaller liquid droplets can be expected to achieve larger supercoolings, on the average, prior to nucleation (if heterogeneous nucleation is limiting supercooling) and to have fewer nuclei. Thus, if a large supercooling is achieved and is maintained during recalescence by the high cooling rate, then it is conceivable that a spherical front growth with segregationless solidification has resulted. This would result in a supersaturated solid solution from which the small (100 to 500 Å) precipitates would be expected to form. Fields of these precipitates have been observed in TEM, but no definitive work has been done. The particle of Fig. 3 was one such field where there were only small precipitates present in a non-cellular grain-boundary-less field of view.

It appears that the RSP powder material is locally very homogeneous. The consolidation process would tend to reduce any segregation present by deformation of the structure. The RSP consolidated material, then, should be locally homogeneous. This has been demonstrated in the chemical profile near the grain boundary region in the consolidated material. Due to the nature of the powder processing of this study, it is expected that the RSP consolidated material is also chemically homogeneous on a macroscale. This has not been conclusively demonstrated. The chemical information across the grain boundary in the conventionally processed material demonstrates that this grain boundary is free of any significant segregation. Although this composition profile extended 5 microns across the material it should be noted that any segregation associated with the solidification of the conventionally processed material would probably be present on a larger scale than that being observed here. For instance, if the average spacing between the large cigar-shaped precipitates is taken as a measure of the distance over which segregation can be expected, then it is necessary to look over distances on the order of 50 microns, a job better suited to the electron microprobe. Investigation of the long range homogeneity of the RSP consolidated material could also be pursued in this way.

The grain growth resistance of the RSP material relative to that of the conventionally processed material appears to be associated with the highly uniform dispersion of small (100 to 500 Å) precipitates in the RSP material. These hinder boundary motion and hence grain coarsening. Note that no small [illegible]

precipitates have been observed in the conventionally processed material and this material exhibits accelerated grain growth relative to the RSP material. It is also possible that the chemical homogeneity of the RSP material plays a role in the retarded grain growth behavior observed.

The observations on the high-phosphorus stainless steel have provided a perspective with which to view both the structural characteristics of the 303 stainless steel and the experimental approach of this study. The highly regular cellular structure of the high phosphorus stainless steel RSP powder stands in marked contrast to the non-regular cell structure of the 303 stainless steel RSP powder and illustrates well the variability of obtainable structures in RSP. The second phase morphology of the high-phosphorus stainless steel suggests a dependence of the precipitate morphology on the relative surface energies of precipitate and matrix and that a higher value for this parameter exists in the 303 stainless steel compared with the high-phosphorus stainless steel. Note the rapid decrease of the phosphorus signal (and, indeed, the nickel and chromium signals) within 500 A of the cell wall. The information and resolution in this and other similar profiles demonstrates not so much the resolving power of the instrument but its applicability to observation of the fine-scale chemical variations encountered in material structures such as these rapidly solidified metal alloys.

CONCLUSIONS

Rapid solidification processing of a high-sulphur austenitic type 303 stainless steel produces a significant refinement in the microstructure and microchemistry of the material. Hot extrusion of the RSP powder retains the beneficial microchemical effects of RSP while refining the grain structure through deformation. Dedicated scanning transmission electron microscopy is an effective experimental approach to detailed analysis of the microstructural and microchemical nature of rapidly solidified metal alloys.

ACKNOWLEDGMENTS

The authors wish to thank Professor M. Cohen and Dr. G. B. Olson for many valuable discussions. This work was supported by the Office of Naval Research, Contract No. N00014-76-C-0171; NR0 31-795.

REFERENCES

1. D. J. Looft and E. C. Van Reuth, Proceedings of the International Conference on Rapid Solidification Processing, Reston, Virginia, November 1977, Claitor's Publishing Division, Baton Rouge, 1978.
2. R. D. Field and H. L. Fraser: Met. Trans. 9A, 131 (1978).
3. J. P. Hirth: Met. Trans. 9A, 401 (1978).
4. G. A. Colligan and B. J. Bayles: Acta Met. 10, 895 (1962).
5. J. Baker and J. W. Cahn: "Solidification," ASM Seminar Book (1969).